Atmos. Chem. Phys. Discuss., 8, 17393–17422, 2008
www.atmos-chem-phys-discuss.net/8/17393/2008/
© Author(s) 2008. This work is distributed under
the Creative Commons Attribution 3.0 License.

Atmospheric Chemistry and Physics Discussions

This discussion paper is/has been under review for the journal *Atmospheric Chemistry and Physics (ACP)*. Please refer to the corresponding final paper in *ACP* if available.

Temporal trends of anthropogenic SO_2 emitted by non-ferrous metal smelters in Peru and Russia estimated from Satellite observations

M. F. Khokhar[1,*], **U. Platt**[2], **and T. Wagner**[1,2]

[1]Institute for Environmental Physics, University of Heidelberg, Heidelberg, Germany
[2]MPI for Chemistry (Otto Hahn Institute), Mainz, Germany
[*]now at: Service d'Aéronomie Université Pierre et Marie Curie, Paris, France

Received: 5 August 2008 – Accepted: 21 August 2008 – Published: 18 September 2008

Correspondence to: M. F. Khokhar (khokhar@aero.jussieu.fr)

Published by Copernicus Publications on behalf of the European Geosciences Union.

Abstract

We report on satellite observations of atmospheric Sulfur Dioxide (SO_2) emitted from metal smelting industries in Peru, South America and Siberia, Russia. Most of the non-ferrous metal ores are sulfidic and during the smelting process the sulfur is emitted as SO_2. In addition to Norilsk, Russia, Peruvian copper smelters are among the most polluting point sources in the world. We retrieve SO_2 column amounts from spectra of the Global Ozone Monitoring Experiment (GOME) on the Earth Research Satellite 2 (ERS-2) for the years 1996 to 2002 using an algorithm based on differential Optical Absorption Spectroscopy (DOAS). Areas of enhanced SO_2 column amounts are clearly identified on a 7-years mean map of GOME observations over the regions with La Oroya and Ilo copper smelters of Peru and Norilsk smelters of Russia.

Since the instrument sensitivity is highly dependent on surface albedo, SO_2 vertical profile, solar zenith angle (SZA), wavelength, clouds, and aerosol, radiative transfer modelling is used to convert the analysed slant column densities into vertical column densities. In this study, the full spherical Monte-Carlo radiative transport model TRACY-II is used for SO_2 AMF calculation.

GOME data is analysed in further detail by calculating time series over these regions. For the different locations, the results demonstrate both, increasing and decreasing trends in the SO_2 column amounts over the time period of 1996–2002. The decreasing trend for the Ilo copper smelter is in good agreement with implemented measures for emission reductions. However, even for the cases with decreasing trends, these point sources are still a dominant source of anthropogenic SO_2 emissions in their region. For the smelters in Peru, the potential influence due to SO_2 emission by the nearby volcanoes is investigated and found to be negligible.

ACPD

8, 17393–17422, 2008

1 Introduction

Sulfur is prevalent in metal ores that contain common metals like aluminium, copper, zinc, lead, nickel, iron etc. For instance, copper is found in the earth's crust primarily as chalcopyrite ($CuFeS_2$), with other sulphide ores, such as bornite (Cu_5FeS_4), covellite (CuS) and chalcocite (Cu_2S), and oxide ores (CuO) (EET, 1999). The reduction of the metal ion to the free metal is normally accomplished in a process referred to as smelting. As a result sulfur in the metal ore is eliminated as sulfur dioxide (SO_2).

Sulfur dioxide emissions occur in significant amounts at various processes associated with metal smelting. Its release into the atmosphere occurs primarily during material handling operations (Fugitive Emissions), and during smelting processes gases are exhausted through stack (Point Source or Stack Emissions). Recovery of SO_2 – usually the hot gases are piped to an acid plant for the manufacturing of sulfuric acid before exhausting them through a stack (EET, 1999) – is a good environmental practice (adopted in several industrialized countries) and may be economically beneficial.

Global SO_2 emissions are mainly of anthropogenic origin and contribute about 76 Mt S/yr, mainly from fossil fuel consumptions and industrial activities with 68 Mt S/yr from Northern Hemisphere and 8 Mt S/yr from Southern Hemisphere (Benkovitz et al., 1996). SO_2 emitted from smelters has severe effects on forest, vegetation, land surface, and water reservoirs in the close vicinity of the smelters (EET, 1999; Aamlid, 2002; AMAP, 2006; Savard et al., 2006; Telmer et al., 2006). Especially; forests near large sources are severely damaged. Symptoms are recognized on Scots pine (Pinus sylvestris) and downy birch (Betula pubescens) and on other plants, e.g. dwarf birch (Betula nana) and Bilberry (Vaccinium myrtillus) (Aamlid, 2002; AMAP, 2006).

Telmer et al. (2006) stated during the study of 99 lakes around the Horne smelter (See Table 1) in Québec that lakes within 50 km of the smelter have elevated metal concentrations in their near-surface sediments due to stack emissions. Therefore, the study of emissions in the environment around smelters is a priority in evaluating policies in relation to a sustainable development.

ACPD
8, 17393–17422, 2008

Satellites provide the best platform to monitor environmental hazards on global scales over extended periods of time. GOME observations during 1996–2002 showed significant amount of anthropogenic SO_2 around the globe mainly from industrial regions such as USA, China, Eastern Europe, South Africa, Canada, Chile, Japan, Peru, and particularly from Siberia, Russia (Khokhar et al., 2004; Khokhar, 2006).

A database presented in Table 1 shows the information about Cu smelters (selection mainly based on their production capacities) from mostly polluted and industrialised region around the world. This work will focus on SO_2 emissions from Peruvian Cu smelters La Oroya, Ilo and from Norilsk smelters in Siberia, Russia.

2 Data analysis

Over the last decades, the potential of remote sensing measurements on satellite platforms was increasingly used to analyze various parameters of the state of the earth, e.g. daily weather, magnetic field, topography, land cover, ocean waves or temperature. Satellite data has also successfully been used to analyze the chemical composition of the atmosphere by measuring spectra of the light reflected (or emitted) by the earth's surface and atmosphere. Such measurements are performed by instruments using different spectral ranges (e.g. UV, visible, IR, and microwave) and viewing geometries, with different potentials and limitations. Additionally, satellite instruments have the advantage of being able to observe the whole globe with the same instrument on a long timescale. Thus, it is possible to gain important details of long-term temporal evolutions and global variability of the atmospheric state.

In 1995, the Global Ozone Monitoring Experiment (GOME), a nadir-scanning UV-VIS spectrometer, was launched on ERS-2 into a near-polar sun synchronous orbit at a mean altitude of 790 km with a local equator crossing time at 10:30 a.m. (Burrows et al., 1999). Total ground coverage is obtained within 3 days at the equator by a 960 km across-track swath. For the measurements presented in this work, the ground pixel size is 40 (along track) by 320 (across track) km^2. As suggested by its name, GOME was

ACPD
8, 17393–17422, 2008

originally designed for the monitoring of (mainly stratospheric) ozone. However, the instrument proved to be extremely useful for the determination of many tropospheric trace gases, like e.g. H_2O, BrO, CH_2O, NO_2 and SO_2 (e.g. Platt et al., 1994; Wagner et al., 2001 etc.).

GOME measures the direct solar spectrum (irradiance) and the Earthshine radiance, i.e. the sunlight reflected by the earth's surface or scattered back by molecules and aerosols in the atmosphere (Burrows et al., 1999). From the ratio of earthshine radiance and solar irradiance measurements, slant column densities (SCD) of the respective absorbers can be derived by applying the technique of differential optical absorption spectroscopy (DOAS) (Perner and Platt, 1979; Platt et al., 1994; Richter et al., 1998a, b; Wagner et al., 2001, 2008). For the SO_2 evaluation we made use of the spectral range from about 312 nm to 327 nm where the strongest bands of the $A^1B_2 \leftarrow X^1A_1$ transition are located. The SCD is the integrated concentration along the light path. For the conversion of the measured SO_2 SCD into the vertical column density (VCD: concentrations integrated vertically) usually an air mass factor (AMF) is applied, which is the ratio of the SCD and the VCD. The AMF can be determined from the numerical simulation of the atmospheric radiative transfer. Also so called Box-AMF can be calculated as the ratios of partial SCD and VCD for different altitude layers. They describe the altitude dependence of the sensitivity of the satellite observation.

3 Radiative transfer modelling

In case of SO_2, the calculation of an appropriate AMF is complicated by several factors: First the SO_2 AMF depends strongly on the SO_2 profile, which largely differs for the different types of sources like e.g. fugitive emissions, industrial plants, or Volcanoes (Richter et al., 2002a; Khokhar et al., 2005; Khokhar, 2006). Furthermore, the AMF also strongly depends on the surface albedo, clouds, SZA and aerosol loading. Information about all these parameters is usually not available for a given GOME SO_2 analysis (Khokhar, 2006). Even in the absence of aerosol as result of the strong

CC BY

Rayleigh scattering in the UV, the measurement sensitivity decreases strongly towards the surface over dark scenes (i.e. at low surface albedo). A sensitivity study on SO_2 AMF calculations presented in (Khokhar et al., 2005) proposed to apply an average AMF of unity. This means that on average the SO_2 VCD actually equals the retrieved SCD. This simplification can be useful e.g. for trend analysis, but in individual cases large deviations from an AMF of about unity can occur, depending especially on cloud cover and surface albedo. Below, we present detailed radiative transfer simulations to exploit the range of possible AMFs relevant for this study.

The calculation of appropriate AMFs for satellite observations of tropospheric SO_2 was investigated in several studies, for instance Thomas et al. (2004), Richter et al. (2002a) and Khokhar et al. (2005, 2006). Here, the full spherical Monte-Carlo model TRACY-II model is used for SO_2 AMF calculations (Deutschmann and Wagner, 2007; Wagner et al., 2007). To account for all aforementioned effects several specific cases were modelled. Sample results presented in Fig. 1 (right panel) show that the SO_2 AMF (for the vertical profile shown in Fig. 1 (left panel) (Taubman et al., 2006) strongly depends on surface albedo, SZA, and the presence of aerosols. The instrument sensitivity towards tropospheric SO_2 expressed as Box-AMF, for different surface albedi is given by Fig. 1 (left panel). The calculations are performed for a wavelength of 315 nm, a SZA of 40°, an aerosol extinction profile as shown in Fig. 1 (see Frieß et al., 2005), single scattering albedo (SAA) of 0.95, an asymmetry parameter g=0.68, surface albedo of 5% (dark surface, solid gray line) and 50% (bright surface, gray line with crosses). As shown in Fig. (1), for bright surfaces (e.g. over snow and ice) much higher sensitivity than for dark surfaces is found. The anthropogenic emission sources investigated in this study are located near the Earth's surface, therefore the main effect of clouds is to shield the resulting enhanced SO_2 concentrations from view and thus lower the sensitivity. Therefore, in this study clouds are assumed at an altitude of 4 km. In Table 2 and Fig. 1 (left panel) different parameters are summarized for TRACY-II simulation runs to calculate SO_2 AMF for specific cases; the resulting AMF are presented in Fig. 1 (right panel).

In order to account for partial cloud cover, the independent pixel approximation (Eq. 1) is used: The SO_2 AMF, A for the total ground pixel is the average of the SO_2 AMF for its clear and for the cloudy parts (weighted by their geometrical fractions and their respective top of atmosphere radiances).

$$A_{\text{total}} = \frac{A_{\text{cloudy}} \cdot f \cdot I_{\text{cloudy}} + A_{\text{clear}} \cdot (1 - f) \cdot I_{\text{clear}}}{f \cdot I_{\text{cloudy}} + (1 - f) \cdot I_{\text{clear}}} \quad (1)$$

Where f denotes the effective cloud fraction of the satellite observation, and I_{cloudy} and I_{clear} the modelled radiances for the cloudy and clear part of the pixel, respectively.

For average effective cloud fraction is assumed 30%, for the observations over Peru and in summertime over Norilsk a surface albedo of 5% is assumed, for the wintertime observations over Norilsk a surface albedo of 80% is assumed. The resulting AMFs for these assumptions are termed as AMF_CCorrec_summer and AMF_CCorrec_winter respectively, and are also shown as a function of SZA in right panel of Fig. (1). These AMFs are used for the conversion of SO_2 SCD into SO_2 VCD in this study.

It should be noted that for many individual cases, these assumptions might differ from reality. Nevertheless, they might well describe the average situation. Since in this study we are interested in average distributions and relative trends, the detailed choice of the assumed parameters will not critically influence the results. From the comparison of the summer and winter results over Norilsk, Siberia, it is found that the chosen parameters lead to consistent results (see below). Also the good agreement of our data with emissions estimated using other methods confirms the suitability of the chosen parameters (see Sect. 4.5). The resulting SO_2 VCD over the Cu smelters of Peru and Russia with possible influence from other sources and their temporal analysis is presented in the following sections.

ACPD
8, 17393–17422, 2008

4 Results

Significant anthropogenic sources of sulphur emissions, and to a lesser extent nitrogen emissions, exist within the arctic region (AMAP, 2006). Sulfuric acid is the most important acidifying substance in the Arctic, with nitric acid being of secondary importance. Industry situated on the Kola Peninsula and Taimyer Peninsula (Russia), nickel and copper processing works in Nikel, Norilsk, Zapolyarnij and Monchegorsk, are the main contributors to the environmental problems due to the emanating air pollution.

Norilsk and Nikel expanded their presence in international markets during the 1990s, remaining Russia's largest source of air pollution and one of the largest trans-boundary emitters of sulfur in Europe (Barrett, 2000). According to AMAP (1998, 2006), Norilsk, contributes significantly to SO_x (SO_2, SO_4^{-2}) emissions above Arctic Circle.

The Cu smelters in Peru are among the most polluting non-volcanic sources of SO_2 in the world. From GOME observations especially the La Oroya and Ilo Cu smelters are found to be strong sources of anthropogenic SO_2 in Peru; they can be clearly identified from 7-years mean map of GOME observations presented in Fig. (4).

4.1 1st case study – Norilsk, Siberia, Russia

Since 1971, nickel and copper from the Norilsk ores in Siberia has been processed in smelters. The Norilsk ore contains more sulfur than the ore produced by the Nikel mine (Tommervik et al., 1995; Michelutti et al., 2001; Aamlid, 2002). In total, Norilsk produces over 90 percent of Russia's nickel, 58 percent of copper, over 80 percent of cobalt and almost 100 percent of the platinum-group metals. By the end of 1997, Norilsk exported 95 percent of its copper and nickel (3% of copper and 23% of nickel of the world's total) to the world markets.

Norlisk, Russia's largest exporter of copper, nickel and other non-ferrous metals, is a well-documented example of a major polluter (Kotov and Nikitina, 1996; Michelutti et al., 2001). According to (Carn et al., 2004), SO_2 emissions from Norilsk are variously reported as being on the order of 2 to 3 megatons (Mt) each year (e.g., Foreign

ACPD
8, 17393–17422, 2008

and Commonwealth Office, Environmental problems in the Russian federation, London Oct 2000, available at: www.fco.gov.uk/Files/kfile/russiaenviro.pdf). However, the emissions estimated in this study from GOME observations over the Norilsk region are 1.685±0.3 Mt SO_2 per year (4.61 kt/day on average) are quite close to the range reported by Foreign and Commonwealth Office, Environmental report about Russia (see also Sect. 4.5). SO_2 emissions from Norilsk smelters (69° N, 88° E), have been consistently detected by GOME instrument since 1996, as can be clearly identified from 7-years mean map of SO_2 VCD for 1996–2002 presented in Fig. 2. GOME observations demonstrate that maximum SO_2 column amounts are found in the vicinity of the Norilsk smelters with a SO_2 plume extending over the surrounding areas as well.

4.2 Temporal analysis of the SO_2 levels in the Norilsk area

GOME observations over the Norilsk region were analyzed in further detail, and a time series over 7-years is presented in Fig. (3). An area (85° E–92° E and 68° N–72° N) was selected and the weekly SO_2 VCD occurring within this region for the whole time period (1996–2002) are presented in Fig. 3. After the Polar night (in Polar Regions, the portion of the year when the Sun does not rise above the horizon. Its length changes from twenty hours at the Arctic/Antarctic Circle (latitude 66° 33′ N or S) to 179 days at the North/South Pole) between March and October, when the solar zenith angle is <80° (as data used in this study are for SZA<80°), SO_2 data can be retrieved from GOME observations over Norilsk.

To account for the strong effect of snow on the measurement sensitivity, data about snow cover extension with in selected region (85° E–92° E and 68° N–72° N) was obtained from Rutgers University Global Snow Lab on special request. Further details about snow coverage data can be obtained from their website (http://climate.rutgers.edu/snowcover) or see Robinson and Frei (2000). Transition between snow covered and snow free surface occurs in May, as identified from the snow data. Thus for the trend analysis we skipped the May observations and calculated two separate time series, one for March and April (using the AMF_CCorrec_winter) and one for June to

ACPD
8, 17393–17422, 2008

September (using the AMF_CCorrec_summer).

The SO_2 VCD during 1997–1998 are of the same order of magnitude for both, the March–April and June–September data. This indicates that, although the spread of the data points represents the large influence of changing cloud cover, our average assumptions on cloud cover, aerosol properties and surface albedo might be reasonable. Linear fits are applied to both data sets used in Fig. 3 in order to obtain the temporal trend in the SO_2 column amounts. Results demonstrate a slight temporal decrease of 8.7% and 7.3% in GOME SO_2 VCD over Norilsk region for summer and winter months respectively. Similarly AMAP (2006) reported that significant reductions in emissions from the non-ferrous metal smelters on the Kola Peninsula, and to a lesser extent from the Norilsk smelters in the Russian Arctic have been observed over the time period of 1990–2003. Nevertheless, non-ferrous metal productions still remain the dominant source of SO_2 emissions in addition to energy production plants and mining industries in the Arctic region.

4.3 Second case study – Peruvian Cu smelters

Analysis of GOME data revealed two persistent sources of SO_2 in Peru identified as copper smelters situated at La Oroya and Ilo. The La Oroya smelter (11.53° S, 75.90° W) is located in the central western part of Peru and is run by Doe Run Co. The Ilo smelter (17.63° S, 71.33° W) is located at the southern west coast of Peru and is run by Southern Peru Copper Corp (SPCC). Annual capacities of these smelters in 2002 were reportedly 80 and 300 thousand metric tons, respectively (Feliciano and González, 2003), making Ilo one of the ten largest copper smelters in the world. Therefore, relatively strong SO_2 emissions can be observed from the Ilo site in the GOME mean map for the period 1996 to 2002 (Fig. 4).

During the time period of 1996–2002, Reventador and Tungurahua volcanoes from Ecuador were active and resulting SO_2 emissions are clearly visible in Fig. 4. Although, sensitivity of the satellite instruments towards weak boundary layer SO_2 signal (as compared to volcanic SO_2 signal – different plume heights) is usually limited (Eisinger

ACPD
8, 17393–17422, 2008

and Burrows, 1998; Richter et al., 2002b; Khokhar et al., 2005), our results show that GOME instrument is sensitive enough to be able to identify the SO_2 being emitted from the La Oroya and Ilo smelters. GOME's ability to detect SO_2 emissions efficiently from Peruvian Cu smelters makes it distinct from the other conventional satellite instruments of last decade.

4.4 Temporal analysis over Peru

A temporal analysis of GOME data over the Peruvian Cu smelters, La Oroya and Ilo was made by selecting SO_2 VCD occurring with in these regions: La Oroya (11°–13° S and 75°–78° W) and Ilo (16.5°–18° S and 70°–74° W) for the time period of 1996–2002. The time series presented in Fig. 5 are averaged over ten days and plotted against the time for whole time period. Linear fits, gray lines, are applied to both data sets in order to obtain the trend in SO_2 emissions. Figure 5a showed a temporal increase of 23% for La Oroya copper smelter, while time series presented in Fig. 5b for Ilo copper smelter showed a temporal decrease of 25% in SO_2emissions.

The temporal decrease in SO_2 emissions from Ilo smelters might be due to proper emission control and the installation of sulphuric acid plants at the Ilo smelters. According to Boon et al. (2001), in 1997 Ilo's local authorities began implementing the Ilo Clean Air Project, with support from international organizations including the World Health Organization (WHO) and the International Council for Local Environmental Initiatives (ICLEI). A second plant was installed in 1998. These two sulphuric acid plants now convert 30 percent of SO_2 into sulfuric acid (Boon et al., 2001) almost consistent with the observed decrease in GOME SO_2 column amounts. There is no information about installation of such a plant at La Oroya smelter.

4.5 Estimation of the total SO_2 emissions

From satellite observations, total emissions can be estimated by

(a) integrating the SO_2 VCD over an area around the source, and

ACPD
8, 17393–17422, 2008

(b) assuming an average atmospheric lifetime.

For the first step care should be taken that the emission source of interest is the only significant source within the selected area. The second step, however, is more critical, since the atmospheric lifetime depends on various parameters (e.g. temperature, precipitation, wind) which are difficult to estimate, and which typically vary with time. Nevertheless, in this section we will present a rough estimate of the emissions from the smelters at Norilsk and in Peru. Note that these estimates are completely independent from existing estimates and provide, therefore complementary information. Also from the comparison to existing estimates it is possible to test the assumptions made in Sect. 3. The annual emissions are calculated using the following equation:

$$E_{\text{annual}} = \frac{\int_{\text{area}} V\,da}{\tau} \cdot 365 \quad (2)$$

Where E_{annual} denotes the annual SO_2 emission, V the SO_2 VCD integrated over the selected area, and τ the atmospheric lifetime of SO_2 in days.

We used average VCD for Russian and Peruvian smelters and integrated over area in m^2 for Norilsk region (85°–92° E and 68°–72° N), for Ilo region (16.5°–18° S and 70°–74° W) and for La Orya region (11°–13° S and 75°–78° W). The distance between given latitude and longitudes coordinates for these regions was calculated by using a tool from Nothern Arizona University USA, available online from their website (http://jan.ucc.nau.edu/~cvm/latlongdist.html).

The atmospheric lifetime of SO_2 is highly variable (Stevenson et al., 2003) depending, in particular on altitude of the SO_2 plume and the presence of clouds (Graf et al., 1997; Khokhar, 2006). It is variously reported ranging from 0.6 to 2.4 days for boundary layer anthropogenic emissions (e.g. Atkinsen et al., 1997; Feichter et al., 1997; Graf et al., 1997; Brasseur et al., 1999; IPCC, 2001; Von Glasow et al., 2002; Stevenson et al., 2003; etc.), as compared to volcanic SO_2 lifetime of 6 days which is injected at high altitudes (e.g. Feichter et al., 1997; Graf et al., 1997; etc.). In this study, lifetime of 1 day for anthropogenic SO_2 is assumed. After converting SO_2 VCD (molecules/cm^2) integrated

CC BY

over given area i.e. molecules/area into mass/area ($6.02 \cdot 10^{23}$ molecules equals 64.07 g of SO_2), yearly emissions for the three smelters are derived. For Norilsk smelters, SO_2 emissions of 1.685±0.3 Mt/yr are comparable to existing estimates 2–3 Mt/yr by Carn et al. (2004). The minor differences could be due to either the assumed lifetime being possibly too long and/or the applied SO_2 AMF are slightly too large. Similarly, SO_2 emissions for la Oroya smelter 0.953±0.07 Mt/yr and for Ilo 1.0953±0.2 Mt/yr are close to Carn et al. (2007) estimates for both Peruvian smelters for September 2004–June 2005. However, in general, we conclude that our assumptions made in Sect. 3 are reasonable.

4.6 Regional volcanic eruptions

The South American plate has three principal zones of active volcanism: the Northern Zone (in Ecuador and Columbia), the Central Zone (southern Peru, northern Chile, south-western Bolivia, and north-western Argentina), and the Southern Zone (southern Chile and southern Argentina) (de Silva and Francis, 1991). The northern and southern zones are both relatively well known, at least the identities and locations of the major volcanoes have been documented. By contrast, the Central Volcanic Zone of the Andes remains one of the largest but least known areas of active volcanism in the world. The Central Volcanic Zone of the Andes is located between latitudes 14° and 28° S of the Andean cordillera. This high altitude plateau is mostly consisting of both active and passive volcanoes, much of them over 4000 m in altitude, constituting the Altiplano of Bolivia and Puna of north Chile and Argentina, see Table 3. Since this work focuses on the SO_2 emissions from Peruvian copper smelters, only the information about Peruvian volcanoes from central Andes volcanic zone are presented. Table 3 gives information about the location, type and the last known activities of Peruvian volcanoes. These information were retrieved from bulletins of global volcanism network (BGVN, http://www.volcano.si.edu) and allow investigating any possible influence of volcanic SO_2 emissions to the Peruvian copper smelter SO_2 emissions (as it

ACPD
8, 17393–17422, 2008

happened in case of Hekla eruption – for details see Khokhar, 2006). According to Table 4, only two volcanoes Ubinas and Sabancaya were active during GOME period 1996–2002. Volcanic activities of both volcanoes are discussed in further detail in the following section.

4.6.1 Ubinas volcano

The Ubinas volcano (a stratovolcano with 1300 m altitude) is located about 800 km southeast of the La Oroya copper smelter and about 180 km northeast of the Ilo copper smelter. According to Bulletins of GVN (BGVN, 1996), the Ubinas volcano experienced only a minor eruption/degassing during July 1996 and amount of SO_2 was not sufficient to influence the anthropogenic SO_2 from both smelters.

4.6.2 Sabancaya volcano

The Sabancaya volcano (a stratovolcano with 5967 m altitude), is located just 210 km North-West of the Ubinas volcano, about 675 km South-East of the La Oroya and 213 km North-West of Ilo copper smelters.

According to bulletins of GVN summarized in Table 3, Sabancaya volcano was active 5 times during the GOME period (1996–2002). It is most probable that any strong volcanic eruption may affect the SO_2 VCD observed over the Ilo copper smelter. Efforts are made to avoid the confusion of volcanic plumes with anthropogenic ones by selecting only SO_2 VCD from area strictly confronting the smelter's SO_2 plume and excluding the volcano location. Furthermore, it is investigated by looking on each of its volcanic activity and extents of volcanic plume precisely and skipping the data for days with volcanic activities of Sabancaya. As stated in BGVN (1997), Sabancaya volcano experienced a moderate eruption in the month of May 1997. On 1st and 2nd of May, aviation reports described ash-bearing plumes. The plume on 1 May reportedly reached 5.5-km altitude; the one on 2 May, 7.3-km altitude. GOME observed the Sabancaya volcanic eruption on 2nd of May (missed on 1st of May due to a data gap)

ACPD
8, 17393–17422, 2008

and most likely the data were affected because both, volcano and Ilo copper smelter, typically lie in the same ground pixel (GOME pixel size 320 by 40 km^2). Therefore, this observation was eliminated from the time series. During July 1997, Sabancaya experienced only fumarolic activity (BGVN, 1997).

The GOME instrument observed Sabancaya's volcanic activities efficiently in accordance to GVN bulletins (with the exception of data gaps). However, there was no distinctive evidence found that volcanic SO_2 plume mixed with anthropogenic SO_2 on the basis of the following arguments:

1. Most of the time eruptions were minor and periodic, and lasted only for a few hours.
2. A maximum plume height of only 1 km was reached except on 2 May 1997. (Data was excluded from analysis)
3. The extent of the volcanic plume was not large enough to reach the south westerly extending plume of Ilo smelter, see Fig. 4. Because this is the region of westerly prevailing trade winds, so most of the times the plume drifted northwest or north making it less probable that it affected the Ilo plume (situated south east of the volcano).
4. The time series presented in Fig. 5b did not show any correlation of relatively larger peaks with to these volcanic activities in 1997, 1998 and 2000.

The only reason why volcanic emissions may still affect the results is the coarse spatial resolution of the GOME. But this can only happen if both volcano and smelter lie in the same ground pixel (taking into account also the effects of finite lifetime and wind transport).

ACPD
8, 17393–17422, 2008

5 Conclusions

Satellite remote sensing systems provide a regular and consistent monitoring of the earth, which is invaluable to monitor the earth system and effect of human activities on it. It is a useful tool to obtain information about various atmospheric trace gas emissions and their distribution on a global scale. The GOME instrument on-board ERS-2 enabled the observations of atmospheric SO_2 for more than 7 years. The analysis of GOME data illustrates that it holds plenty of information on the different SO_2 sources, both of anthropogenic and natural origin.

Anthropogenic SO_2 is much more difficult to detect from satellite instruments than volcanic SO_2 because it is generally located at lower altitudes where the instrument's sensitivity is low (Eisinger and Burrows, 1998; Khokhar, 2006). Enhanced anthropogenic SO_2 emissions can be identified from regions with extensive burning of coal, smelting of metal ores and heavy industrial activities

GOME data showed that the emissions from Norilsk can be clearly identified with maximum SO_2 column amonuts during winter and spring. These high values are mainly caused by underlying snow which enhances the earth's albedo (referred to as albedo effect, see Khokhar et al., 2004, 2006). In this study, efforts are made to take the albedo effect into account by using different parameters for SO_2 AMF calculation during winter and summer. The resulting time series of GOME SO_2 VCD from Norilsk showed a consistent seasonal pattern over the time period of 1996–2002 with an overall slightly decreasing trend. This decrease is in good qualitative agreement with AMAP (2006) and other studies. Nevertheless, the Norilsk smelters are still the dominant source of anthropogenic SO_2 emissions in the region.

The total annual emissions derived from our analysis for different regions are close to that of existing estimates (e.g. Common Wealth, AMAP, 2006; Carn et al., 2004, 2007) indicating that our assumptions on the atmospheric radiative transfer and the SO_2 lifetime are reasonable.

GOME's ability to detect weak signals of boundary layer SO_2 from La Oroya and Ilo

ACPD
8, 17393–17422, 2008

copper smelters in Peru allowed an efficient monitoring of SO_2 on a regular basis (with exception of data gaps). Time series calculated for La Oroya and Ilo smelters showed a temporal increase by 23% and a 25% decrease in SO_2 emissions from these non-ferrous smelter, respectively over the time period from 1996 to 2002.

Due to coarse spatial resolution of GOME, it the SO_2 VCD obtained over Peru could in principle have been affected to some extent by the emissions of the nearby Volcanoes Ubinas and Sabancaya as it happened in case of Norilsk during Hekla eruption in 2000 (for details see Khokhar, 2006). However, from careful sensitivity studies, this potential source of interference could be clearly ruled out. Additionally, GOME observations are in good agreement with bulletins of global volcanism network (BGVN).

Satellite remote sensing systems with periodic (global coverage in few days) and consistent monitoring have several advantages over other techniques. They also have some limitations, especially coarse spatial resolution (GOME: 40 by 320 km^2). However, this limitation will be abated by other satellite instruments onboard space missions from ESA and NASA e.g. SCIAMACHY, OMI or GOME-2, which are already in space and have comparably better spatial resolution. The increased spatial resolution will help to monitor, localize, and study SO_2 plumes more precisely and quantify their impact on a finer spatial scale.

Acknowledgements. The authors gratefully acknowledge the financial support and providing of ERS-2, GOME data by DLR (Wessling, Germany) and ESA (Frascati, Italy). We especially acknowledge the GVN Volcanic Emission database from their website http://www.volcano.si.edu/reports/bulletin/ and for snow coverage data Mr. Thomas Estilow from Rutgers University Global Snow Lab. In addition, special thanks to all colleagues for their contribution and tremendous help. We are particularly grateful to T. Deutschmann who developed the Monte-Carlo radiative transfer model TRACY-II.

CNRS CENTRE NATIONAL DE LA RECHERCHE SCIENTIFIQUE INSU

The publication of this article is financed by CNRS-INSU.

References

Aamlid, D.: Air pollution effects in the Norwegian-Russian border area. A status report, Norwegian, Pollution Control Authority (SFT), 34 pp. ISBN 82-7655-446-6, 2002.

AMAP Assessment Report: AMAP (Arctic Monitoring and Assessment Program). Arctic Pollution Issues, Oslo, Norway, Xii, 859 pp., 1998.

AMAP Assessment Report: AMAP (Arctic Monitoring and Assessment Program). Arctic Pollution Issues, Oslo, Norway, ISBN 82-7971-045-0, 2006.

Atkinson, R., Baulch, D. L., Cox, R. A., Hampson Jr., R. F., Kerr, J. A., Rossi, J. A., and Troe, J.: Evaluated kinetic, photochemical, and heterogeneous data for atmospheric chemistry, Supplement V, IUPAC subcommittee on gas kinetic data evaluation for atmospheric chemistry, J. Phys. Chem. Ref. Data, 26, 521–1011, 1997.

Barrett, M.: The Worst and the Best: Atmospheric Emissions from Large Point Sources in Europe, Report of the Swedish NGO Secretariat on Acid Rain, 2000.

Benkovitz, C. M., Scholtz, M. T., Pacyna, J., Tarrason, L., Dignon, J., Voldner, E. C., Spiro, P. A., Logan, J. A., and Graedel T. E.: Global gridded inventories of anthropogenic emissions of sulphur and nitrogen, J. Geophys. Res., 101, 29 239–29 253, 1996.

BGVN: Ubinas, Bulletin of the Global Volcanism Network (BGVN, 21:07), http://www.volcano.si.edu/, 1996.

BGVN: Sabancaya, Bulletin of the Global Volcanism Network (BGVN, 23:07), http://www.volcano.si.edu/, 1997.

BGVN: Sabancaya, Bulletin of the Global Volcanism Network (BGVN, 23:05, 23:08, 23:10), http://www.volcano.si.edu/ 1998.

BGVN: Hekla, Bulletin of the Global Volcanism Network (BGVN, 25:02, 25:06), http://www.volcano.si.edu/ 2000a.

BGVN: Sabancaya, Bulletin of the Global Volcanism Network (BGVN, 25:05), http://www.volcano.si.edu/, 2000b.

Boon, R. G. J., Alexaki, A., and Becerra, E. H.: The Ilo Clean Air Project: A local response to industrial pollution control in Peru, Environ. Urbanization, 13(2), 215–232, 2001.

Brasseur, G., Orlando, J., and Tyndall, G.: Atmospheric chemistry and global change. Chapter No: 5, Trace gas Exchanges and biogeochemical sulfur cycles, Oxford Univ. Press, New York, 195–200, ISBN-10: 0195105214, 1999.

Burrows, J., Weber, M., Buchwitz, M., Rozanov, V., Ladstetter-Weißenmayer, A., Richter, A.,

ACPD

8, 17393–17422, 2008

De Beek, R., Hoogen, R., Bramstedt, K., Eichmann, K. U., Eisinger, M., and Perner, D.: The Global Ozone Monitoring Experiment (GOME): Mission concept and first scientific results, J. Atmos. Sci., 56, 151–175, 1999.

Carn, S. A., Krueger, A. J., Krotkov, N. A., and Gray, M. A.: Fire at Iraqi sulfur plant emits SO_2 clouds detected by Earth Probe TOMS, Geophys. Res. Lett., 31, L19105, doi:10.1029/2004GL020719, 2004.

Carn, S. A., Krueger, A. J., Krotkov, N. A., Yang, K., and Levelt, P. F.: Sulfur dioxide emissions from Peruvian copper smelters detected by the Ozone Monitoring Instrument, Geophys. Res. Lett., 34, L09801, doi:10.1029/2006GL029020, 2007.

De Silva, S. L. and Francis, P. W.: Volcanoes of the Central Andes, published by Springer-Verlag, 216 pp., 1991.

Deutschmann, T. and Wagner, T.: TRACY-II Users manual, (http://www.mpch-mainz.mpg.de/satellite/), 2007.

EET (Emission Estimation Technique): Manual for Copper Concentrating, Smelting and Refining, National Pollutant Inventory, Environment Australia, 1999.

Eisinger, M. and Burrows, J. P.: Tropospheric Sulfur Dioxide observed by the ERS-2 GOME Instrument, Geophys. Res. Lett., 25, 4177–4180, 1998.

Feichter, J., Lohmann, U., and Schult, I.: The atmospheric sulphur cycle in ECHAM-4 and its impact on the shortwave radiation, Clim. Dynam., 13, 235–246, 1997.

Feliciano, C. S. L. and Gonzalez, E.: Map and table of world copper smelters, US Geol. Surv. Open File Rep., 03-075, http://pubs.usgs.gov/of/2003/of03-075/index.html, 2003.

Frieß, U., Wagner, T., Remedios, J. J., Monks, P. S., Sinreich, R., and Platt, U.: Retrieval of aerosol properties with Multi-axis DOAS, poster, ACCENT symposium Urbino, September 2005.

Graf, H.-F., Feichter, J., and Langmann, B.: Volcanic sulphur emissions: Estimates of source strength and its contribution to the global sulphate distribution, J. Geophys. Res., 102, 10 727–10 738, 1997.

IPCC: Intergovernmental Panel on Climate Chang: The Scientific Basis, chapter 5; in: Aerosols, their Direct and Indirect Effects, edited by: Andreae, M., Annegarn, H., Barrie, L., et al., 290–335, Cambridge Univ. Press, NY, 2001.

Khokhar, M. F., Frankenberg, C., Hollwedel, J., Beirle, S., Kühl, S., Grzegorski, M., Wilms-Grabe, W., Platt, U., and Wagner, T.: Satellite remote sensing of atmospheric SO_2: Volcanic eruptions and anthropogenic emissions, Proceedings of the ENVISAT & ERS Symposium,

6–10 September 2004, Salzburg, Austria, ESA publication SP-572, (CD-ROM), 2004.
Khokhar, M. F., Frankenberg, C., Beirle, S., Kühl, S., Van Roozendael, M., Richter, A., Platt, U., and Wagner, T.: Satellite Observations of Atmospheric SO_2 from Volcanic Eruptions during the Time Period of 1996 to 2002, J. Adv. Space Res., 36, 5, 879–887, doi:10.1016/j.asr.2005.04.114, 2005.
Khokhar, M. F.: Retrieval and Interpretation of Tropospheric SO_2 from UV/ VIS Satellite Instruments, PhD thesis, submitted to Faculty of Physics and Geosciences, University of Leipzig, Germany, 2006.
Nikitina, E. and Kotov, V.: Reorganization of Environmental Policy in Russia: The Decade of Success and Failures in implementation and Perspective Quests, Working paper of FEEM (Fondazione Eni Enrico Mattei), accessed via http://papers.ssrn.com/sol3/papers.cfm?abstract_id=318685, 2002.
Michelutti, N., Laing, T. E., and Smol, J. P.: Diatom Assessment of Past Environmental Changes in Lakes Located Near the Noril'sk (Siberia) Smelters, J. Water Air Soil Pollut., 125, 1–4, 231–241(11) by Springer, 2001.
Perner, D. and Platt, U.: Detection of nitrous acid in the atmosphere by differential optical absorption, Geophys. Res. Lett., 7, 1053–1056, 1979.
Platt, U.: Differential Optical Absorption Spectroscopy (DOAS), in: Air Monitoring by Spectroscopic Techniques, edited by: M. W. Sigrist, Chemical Analysis Series, 127, John Wiley, New York, 1994.
Richter A., Eisinger, M., Ladstätter-Weißenmayer, A., and Burrows, J. P.: DOAS zenith sky observations. 2. Seasonal variation of BrO over Bremen (53° N), 1994–1995, J. Atmos. Chem., 1998a.
Richter A., Wittrock, F., Eisinger, M., and Burrows, J. P.: GOME observations of tropospheric BrO in northern hemispheric spring and summer 1997, Geophys. Res. Lett., 25, 2683–2686, 1998b.
Richter, A., Wittrock, F., Ladstätter-Weißenmayer, A., Burrows, J. P., and Arlande, D. W.: GOME Measurements of SO_2, Poster at the DPG Tagung, 2002a.
Richter A., Wittrock, F., Ladstätter-Weißenmayer, A., and Burrows, J. P.: GOME measurements of stratospheric and tropospheric BrO, J. Adv. Space Res., 29(11), 1667–1672, 2002b.
Robinson, D. A. and Frei, A.: Seasonal variability of Northern Hemisphere snow extent using visible satellite data, Prof. Geogr., 51, 307–314, 2000.
Savard, M. M., Bonham-Carter, G. F., and Banic, C. M.: A geoscientific perspective on air-

borne smelter emissions of metals in the environment: an overview, Geochem., 6, 99–109, doi:10.1144/1467-7873/05-095, 2006.
SPCC: Southern Peru Copper Corp dedicates new plant at Ilo - SPCC adds sulphuric acid plant at Ilo smelter, Brief Article [see webpage http://sec.edgar-online.com/1997/03/28/00/0000007649-97-000005/Section2.asp], EDGAR online Inc., 28 March, 1997
Stevenson, D. S., Johnson, C. E., Highwood, E. J., Gauci, V., Collins, W. J., and Derwent, R. G.: Atmospheric impact of the 1783–1784 Laki eruption: Part I Chemistry modelling, Atmos. Chem. Phys., 3, 487–507, 2003, http://www.atmos-chem-phys.net/3/487/2003/.
Taubman, B. F., Hains, J. C., Thompson, A. M., Marufu, L. T., Doddridge, B. G., Stehr, J. W., Piety, C. A., and Dickerson, R. R.: Aircraft vertical profiles of trace gas and aerosol pollution over the mid-Atlantic United States: Statistics and meteorological cluster analysis, J. Geophys. Res., 111, D10S07, doi:10.1029/2005JD006196, 2006.
Telmer, K. H., Daneshfar, B., Sanborn, M. S., Kliza-Petelle, D., and Rancourt, D. G.: The role of smelter emissions and element remobilization in the sediment chemistry, Geochem., 6, 187–202, 2006.
Thomas, W., Erbertseder, T., Ruppert, T., Van Roozendael, M., Verdebout, J., Balis, D., Meleti, C., and Zerefos, C.: On the retrieval of volcanic sulfur dioxide emissions from GOME backscatter measurements, J. Atmos. Chem., 50, 3, doi:10.1007/s10874-005-5544-1, 295–320, 1–26, 2004.
Tommervik, H., Johansen, B. E., and Pedersen, J. P: Monitoring the effects of air pollution on terrestrial ecosystems in Varanger (Norway) and Nikel-Pechenga (Russia) using remote sensing, Sci. Total Environ., 160/161, 753–767, 1995.
Von Glasow, R., Sander, R., Bott, A., and Crutzen, P. J.: Modeling halogen chemistry in the marine boundary layer. 2. Interactions with sulfur and the cloud-covered MBL, J. Geophys. Res., 107 (D17), 4323, doi:10.1029/2002JD000943, 2002.
Wagner, T., Leue, C., Wenig, M., Pfeilsticker, K., and Platt, U.: Spatial and temporal distribution of enhanced boundary layer BrO concentrations measured by the GOME instrument aboard ERS-2, J. Geophys. Res., 106, 24 225–24 236, 2001.
Wagner, T., Burrows, J. P., Deutschmann, T., Dix, B., von Friedeburg, C., Frieß, U., Hendrick, F., Heue, K.-P., Irie, H., Iwabuchi, H., Kanaya, Y., Keller, J., McLinden, C. A., Oetjen, H., Palazzi, E., Petritoli, A., Platt, U., Postylyakov, O., Pukite, J., Richter, A., van Roozendael, M., Rozanov, A., Rozanov, V., Sinreich, R., Sanghavi, S., and Wittrock, F.: Comparison of box-air-mass-factors and radiances for Multiple-Axis Differential Optical Absorption Spectroscopy

(MAX-DOAS) geometries calculated from different UV/visible radiative transfer models, Atmos. Chem. Phys., 7, 1809–1833, 2007, http://www.atmos-chem-phys.net/7/1809/2007/.
Wagner, T., Beirle, S., Deutschmann, T., Eigemeier, E., Frankenberg, C., Grzegorski, M., Liu, C., Marbach, T., Platt, U., and Penning de Vries, M.: Monitoring of atmospheric trace gases, clouds, aerosols and surface properties from UV/vis/NIR satellite instruments, J. Opt. A, Pure Appl. Opt., 10 (2008), 104019 (9 pp.), doi:10.1088/1464-4258/10/10/104019, 2008.

Table 1. Database of Cu smelters from different countries based on their production capacity*.

Name	Country	Latitude (° N)	Longitude (° E)	Capacity (Ktons/yr)	Process Type
Pirdop	Bulgaria	42.7	24.18	190	Outokumpu Flash
Noranda, Horne, Quebec	Canada	48.25	−79.02	200	Noranda Continuous
Timmins, Ontario	Canada	48.47	−81.33	155	Mitsubishi Continuous
La Negra (Altonorte)	Chile	−23.8	−70.33	165	Noranda Continuous
Chuquicamata	Chile	−22.32	−68.93	500	Outokumpu/Teniente Conv.
El Teniente (Caletones)	Chile	−34.1	−70.33	400	Reverberatory/Teniente Conv.
Daye, Hubei	China	30.08	114.95	150	Noranda Conv./Reverberatory
Guixi, Jiangxi	China	28.28	117.18	250	Outokumpu Flash
Kunming, Yunnan	China	25.04	102.72	230	Isasmelt, Electric
Lunen (Huettenwerke Kayser)	Germany	51.62	7.52	170	Issmelt
Hamburg (Norddeutsche Affinerie)	Germany	53.55	10	420	Outokumpu, Contimelt, Electric
Besshi/Toyo, Ehime	Japan	33.88	133.32	300	Outokumpu Flash
Naoshima, Kagawa	Japan	34.45	134	270	Mitsubishi Continuous
Onahama, Fukushima	Japan	36.95	140.9	348	Reverberatory
Saganoseki, Oita	Japan	33.24	131.87	470	Outokumpu Flash
Tamano, Okayama	Japan	34.48	133.93	263	Outokumpu Flash
Nacozari de Garcia, Sonora (La Caridad)	Mexico	30.37	−109.53	300	Outokumpu/Teniente Conv.
La Oroya	Peru	−11.53	−75.9	80	Reverberatory
Ilo	Peru	−17.63	−71.33	300	Reverberatory/Teniente Conv.
Glogow District (Glogow I)	Poland	51.67	16.08	220	Blast Furnace
Glogow District (Glogow II)	Poland	51.67	16.08	205	Outokumpu Flash
Kirovgrad	Russia	57.44	60.06	150	Reverberatory (S)
Norlisk	Russia	69.34	88.22	400	Reverb and Electric
Phalaborwa	South Africa	−23.98	31.07	135	Reverberatory
Huelva	Spain	37.26	−6.95	320	Outokumpu Flash
Skelleftehamn (Ronnskar)	Sweden	65	21.6	240	Electric (TBRC)
Garfield, Utah	USA	37.75	−111.5	320	Kennecott/Outokumpu
Hayden, Arizona	USA	33	−110.78	210	Inco Flash
Miami, Arizona	USA	33.38	−110.87	180	Isasmelt/Electric

(RLE)=Roast Leach, (S)=secondary smelter, (TBRC)=Top Blown Rotary Converter
(*) table adapted from website http://pubs.usgs.gov/of/2003/of03-075/CSTable.txt

ACPD
8, 17393–17422, 2008

Table 2. TRACY-II scenarios of SO_2 AMF calculations.

SO_2AMF	Wavelength (nm)	Aerosol profiles	SSA	Asymmetry parameter "g"	Surface Albedo %
noAerosol	315	–	–	–	5
Aerosol	315	see Fig. 1	0.95	0.68	5
Clouds 80%	315	Clouds at 4 km	1	0.85	80
Clouds 50%	315	Clouds at 4 km	1	0.85	50
Clouds 5%	315	Clouds at 4 km	1	0.85	5

ACPD
8, 17393–17422, 2008

Table 3. Database of Peruvian Volcanoes – summarized from bulletins of GVN.

Volcano	Location	Elevation (m)	Volcano type	Last Known Eruptions*
ANDAHUA VALLEY	15.42° S–72.33° W	4713	Cinder cones	unknown
AUQUIHUATO, CERRO	15.07° S–73.18° W	4980	Cinder cone	unknown
CASIRI, NEVADOS	17.47° S–69.81° W	5650	Stratovolcano	unknown
CHACHANI, NEVADO	16.19° S–71.53° W	6057	Stratovolcano	unknown
COROPUNA	15.52° S–72.65° W	6377	Stratovolcano	unknown
HUAYNAPUTINA	16.608° S–70.85° W	4850	Stratovolcano	1600
EL MISTI	16.29° S–71.40° W	5822	Stratovolcano	05/1984, 12/1985
QUIMSACHATA	14.20° S–71.33° W	3923	Lava dome	4450 BC (?)
SABANCAYA	15.78° S–71.85° W	5967	Stratovolcano	06/1988, 05/1990, 06/1990, 07/1990, 05/1991, 07/1991, 01/1992, 03/1994, 05/1995,**07/1997**, **05/1998 08/1998 10/1998**, 05/2000, 05/2003, 01/2004
SARA SARA	5.33° S–73.45° W	5522	Stratovolcano	unknown
TICSANI	16.75° S–70.59° W	5408	Lava domes	unknown
TUTUPACA	17.02° S–70.35° W	5815	Stratovolcano	unknown
UBINAS	16.35° S–70.90° W	5672	Stratovolcano	06/1969, 07/1969, 12/1985, 07/1996, 03/2006, 05/2006, 10/2006, 2007
YUCAMANE	17.18° S–70.20° W	5550	Stratovolcano	1902

(*): Information retrieved from GVN Bulletins, see references
(?): not certain

ACPD
8, 17393–17422, 2008

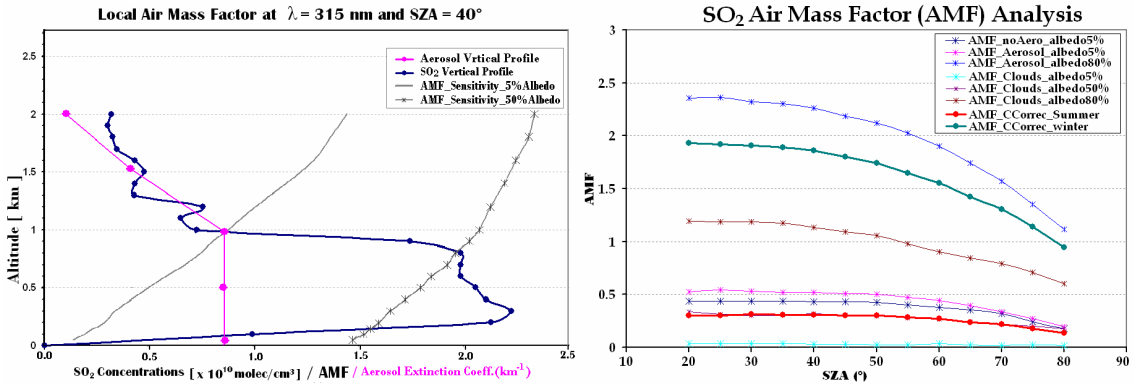

Fig. 1. Left Panel: Vertical profiles of the SO_2 concentration and aerosol extinction coefficient used for AMF calculation. Also shown is the measurement sensitivity (expressed as Box-AMF) towards different surfaces with albedos of 5% (solid Gray line) and 50% (Gray line with cross). Right panel: comparison of SO_2 AMFs for different scenarios. Also shown are selected SO_2 AMF used in this study: AMF_CCorrec_summer (red thick line) used for Norilsk in summer and for Peru, AMF_CCorrec_winter (greenish thick line) used for Norilsk in winter.

ACPD
8, 17393–17422, 2008

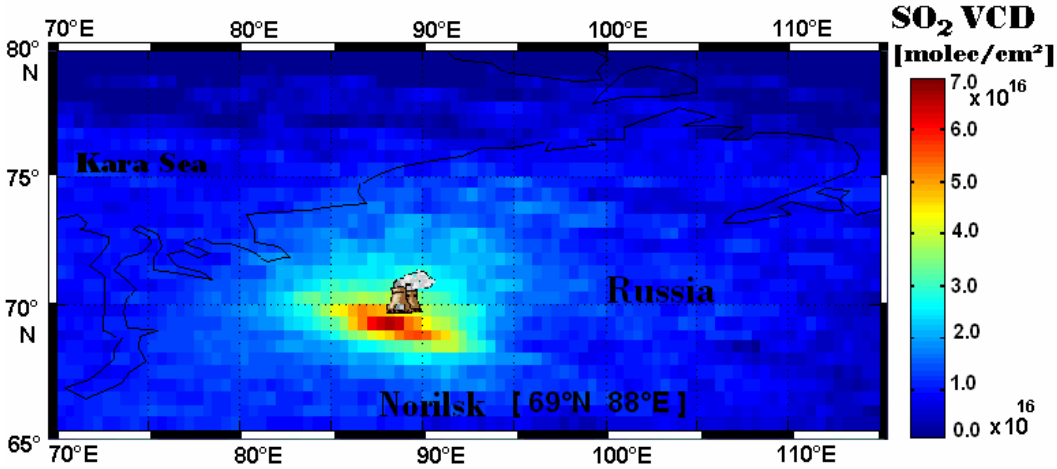

Fig. 2. 7-year (1996–2002) mean map of the SO_2 vertical column density over Norilsk, Russia, showing a strong source of anthropogenic SO_2 emissions. The location of Norilsk copper smelters is indicated by the smoke-stack symbol. Two different AMFs are used for winter and summer months to prepare this mean map (see text).

ACPD
8, 17393–17422, 2008

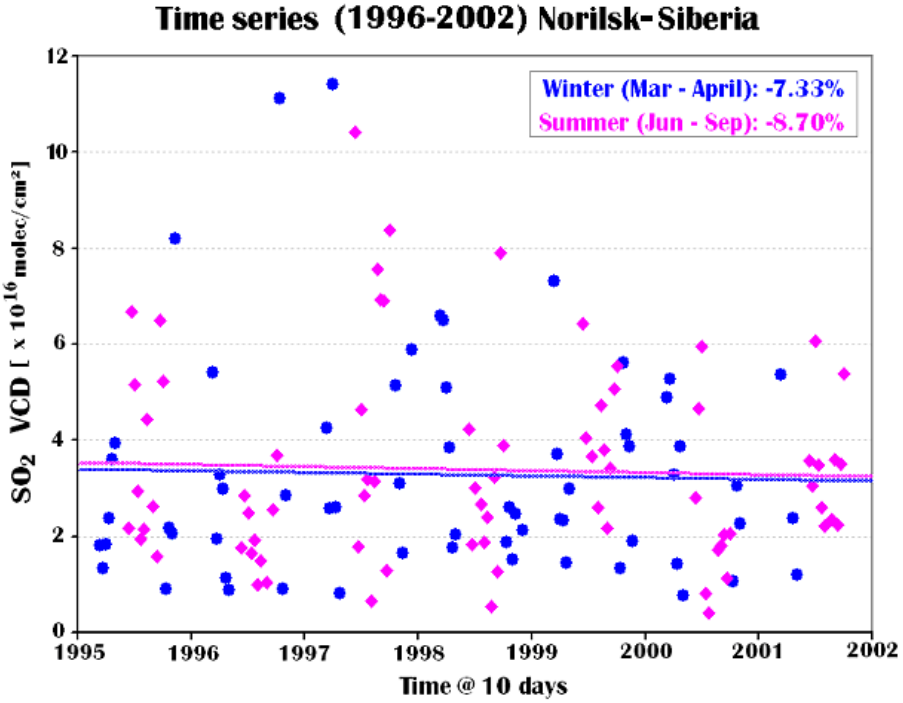

Fig. 3. Time series of the area averaged SO_2 VCD retrieved from GOME data (1996–2002) over Norilsk. Linear fits are applied in order to identify the temporal trend. The spread of the data is mainly caused by variations in cloud cover.

ACPD
8, 17393–17422, 2008

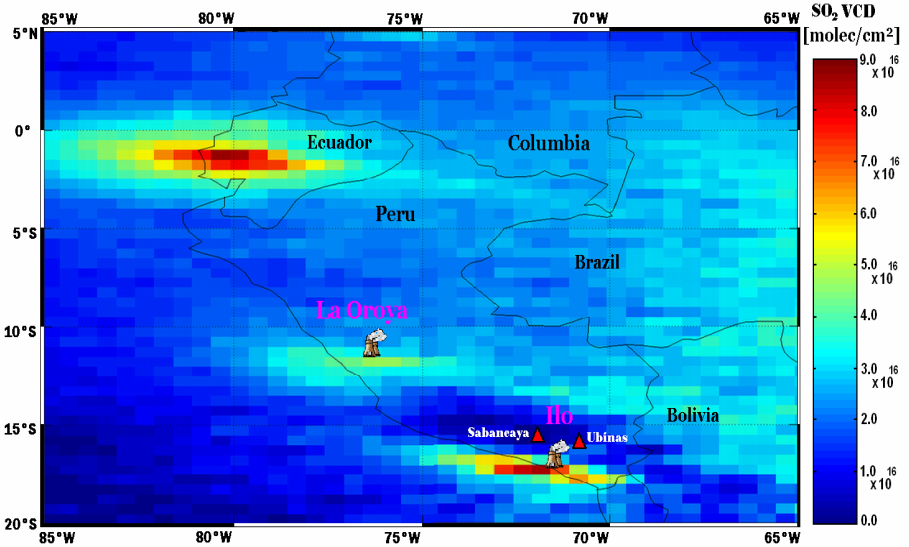

Fig. 4. 7-years (1996–2002) mean map of SO_2 VCD retrieved from GOME data (1996–2002) over Peru and surrounding region. In addition to the hotspots caused by the La Oroya and Ilo Peruvian Cu smelters (indicated by smoke-stack symbols), enhanced SO_2 VCD can also be clearly identified over Ecuador (due to volcanic eruption during this time period).

ACPD
8, 17393–17422, 2008

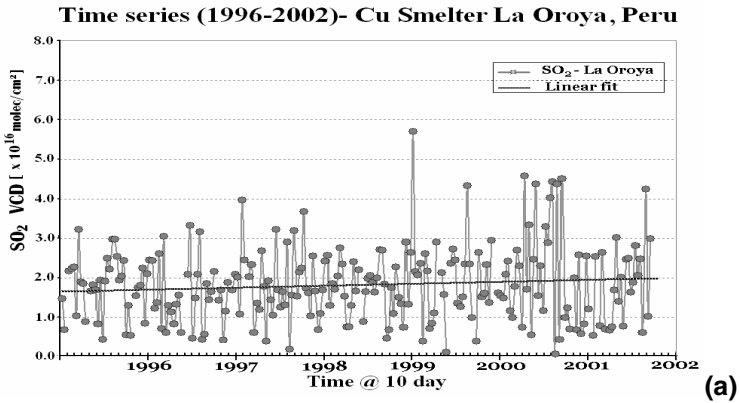

Fig. 5. Time series of the area averaged SO_2 VCD over selected regions over La Oroya **(a)** and Ilo **(b)** Cu smelters, retrieved from GOME data from 1996 to 2002. The individual data points are averages over ten days. Linear fits (Black lines) are applied to both time series. Time Series over La Oroya Cu smelters (a) indicates an increase of 23% while time series over Ilo Cu smelters (b) indicates a decrease of 25%.

ACPD
8, 17393–17422, 2008